TEM studies of laterally overgrown GaN layers grown in polar and non-polar direction

Z. Liliental-Weber[a], D. Zakharov[a], B. Wagner[b], and R.F. Davis[b]
[a]Lawrence Berkeley National Lab, Berkeley, CA;
[b]North Carolina State University, Raleigh, NC 27695

ABSTRACT

Transmission electron microscopy (TEM) was used to study pendeo-epitaxial GaN layers grown on polar and non-polar 4H SiC substrates. The structural quality of the overgrown layers was evaluated using a number of TEM methods. Growth of pendeo-epitaxial layers on polar substrates leads to better structural quality of the overgrown areas, however edge-on dislocations are found at the meeting fronts of two wings. Some misorientation between the "seed" area and wing area was detected by Convergent Beam Electron Diffraction. Growth of pendeo-epitaxial layers on non-polar substrates is more difficult. Two wings on the opposite site of the seed area grow in two different polar directions with different growth rates. Most dislocations in a wing grown with Ga polarity are 10 times wider than wings grown with N-polarity making coalescence of these layers difficult. Most dislocations in a wing grown with Ga polarity bend in a direction parallel to the substrate, but some of them also propagate to the sample surface. Stacking faults formed on the c-plane and prismatic plane occasionally were found. Some misorientation between the wings and seed was detected using Large Angle Convergent Beam Diffraction.

Keywords: lateral overgrowth, polar and non-polar substrates, structural quality, transmission electron microscopy, pendeo epitaxy

1. INTRODUCTION

Major developments in wide-gap III–V nitride semiconductors have recently led to the commercial production of high brightness light emitting diodes (LEDs) with light output from green to near UV [1-5]. LEDs are currently used in traffic lights, color displays, and automotive panel instruments, and use in room lighting is beginning. Pulsed and continued wave (CW) laser diodes (LDs) have been also demonstrated [4,5]. Large dimension native III-nitride substrates are not available. Therefore LED and LD heterostructures are usually grown on (0001) Al_2O_3 or SiC. The large lattice mismatch between these substrates and the GaN layers leads to a high density of defects (mainly dislocations propagating along growth directions and stacking faults formed on c-plane).

The total polarization of nitride films used for devices is aligned along the polar [0001] axis of the wurtzite crystal structure. The direction coincides with the growth direction of the GaN-based layers. This, in turn, causes spontaneous and piezoelectric polarizations within the active layers. Polarization discontinuites along the growth direction create internal electric fields, which spatially separate electrons and holes within the quantum wells. The corresponding red-shift of optical transitions and reduction in oscillator strength have been reported for AlGaN/GaN [6–8] and GaN/In-GaN [9, 10] quantum wells grown along the c-direction. One of the possible solutions to eliminate these undesirable effects is to grow GaN-based epilayers in nonpolar orientations. Without polarization along the growth direction, internal fields should not be present in the active layers. Recently, nonpolar m-plane and a-plane GaN/AlGaN multiple quantum well structures have been grown. The emission was not redshifted and photoluminescence intensity was higher. However, regardless of the growth direction a high defect density is usually observed for all GaN-based layers. These defects are detrimental for the application of these materials for laser diodes.

An established method to decrease the defect density is lateral overgrowth. Two related methods; laterally epitaxial overgrowth (LEO) [11-41] and pendeo-epitaxy (PE) have been developed [15-18]. Application of either of these methods leads to a much lower density of defects, especially those that propagate in the growth direction. In the pendeo-epitaxy method, growth does not initiate through the open windows as it does in LEO structures, but instead it is forced to selectively begin on the sidewalls etched into the seed crystal to form overhanging wings. The details of the growth procedure have been described previously [15,17].

In this paper the structural quality of the GaN overgrown layers (grown on polar and non-polar directions) will be compared based on the results from conventional and high resolution electron microscopy. Specifically, pendeo-epitaxial GaN layers grown originally on 4H-SiC c-plane and r-plane substrate will be compared.
A Topcon 002B electron microscope with 200 KeV acceleration voltage and a JEOL 3010 microscope operated at 300 KeV were used for these studies. A standard **g.b** analysis was used to determine dislocation Burgers vectors. Convergent Beam Electron Diffraction (CBED), or Large Angle CBED (LACBED), was used to determine the tilt/twist angles between wing/wing and wing/seed areas [19-20].

2. EXPERIMENTAL

The PE were deposited onto the etched GaN/AlN seeds (about 1.2 μm in height) which are previously grown on c-plane 4H SiC. The seed height was about 0.15 μm, and the seeds were separated by about 4 μm. The total PE layer thickness between the seeds was measured to be about 3.5 μm. The PE layers grown on 4H-SiC (11$\underline{2}$0) substrates had 100 nm thick AlN buffer layers and 500 nm thick GaN seed layers grown at 20 Torr and temperatures of 1100°C and 1020°C, respectively. A Ni layer was deposited on patterned photoresist stripes on each GaN seed layer by e-beam evaporation. Etch mask stripes were subsequently produced using standard photolithography lift-off techniques. The Ni was then removed using a 5 min dip in 50% HNO_3. The remaining GaN seed layer consisted of 1μm wide stripes oriented along [1$\underline{1}$00] direction separated from each other by 3 μm. The exposed (0001) sidewalls and the top (11$\underline{2}$0) faces of the stripes were subsequently dipped in 50% hot HCl to clean the surface prior to regrowth of the PE layer. Schematic drawings of these samples are shown in Fig. 1. Basically, in PE, etched columnar GaN posts might be capped or not capped with a mask layer. Afterwards, GaN growth proceeds laterally and vertically until it coalesces between and over the mask located on top of the columns, thereby creating a continuous layer. The schematic drawings of the PE layers is shown on Fig. 1.

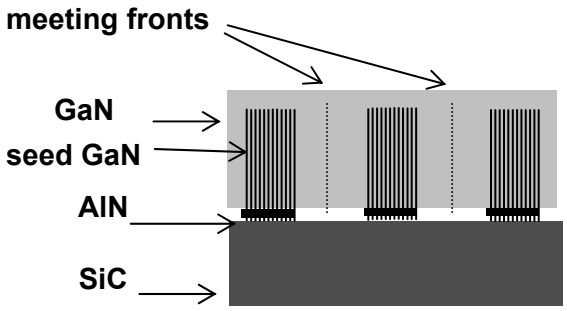

Fig. 1. Schematic diagrams of the pendeo-epitaxial layers. Vertical lines indicate defects in the seed area propagating to the sample surface.

3. RESULTS and DISCUSSION

It was found that defects formed in GaN layers grown on polar and non-polar substrates are different [21]. For the growth in polar direction there are mainly threading dislocations which propagate along the growth direction, but in case of growth in non-polar direction stacking faults are formed on c- planes (growth direction) since their formation energy on these planes is the lowest [22]. Different type of defects present in the seed areas and different crystallographic arrangement of atomic planes will result in substantial difference in the quality of the overgrown wing areas.

Cross-section studies of the PE layers grown on c-plane substrates show that the layer grew sideways from the seed (Fig. 2) and a clear gap was observed between the PE layer and the SiC substrate. Dislocations that were formed in the seeds propagated to the sample surface. Dislocation half-loops are seen to propagate from the seed on the c-planes and their spacing increases with increasing distance from the substrate (Fig. 3a). Large voids were formed at the meeting front of two wings (Fig. 3b). All these voids were overgrown and dislocations were formed in this area of the crystal. Analysis of these dislocations showed that most of them

had screw character.

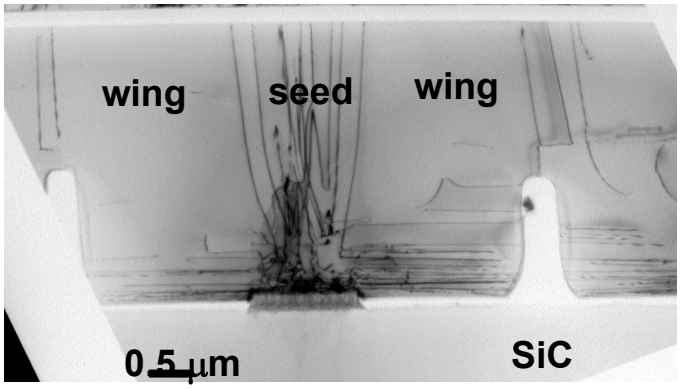

Fig. 2. Cross-section micrograph from the PE sample grown without the mask showing defect distribution over the seed and in the wings. Note the uniform contrast indicating that the misorientation in this sample is small.

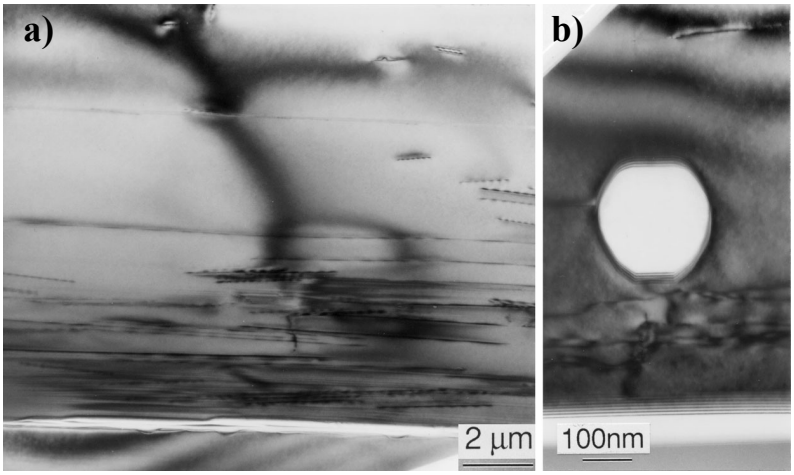

Fig. 3. (a) Dislocation loops formed in the wing area. Note their higher density in the area closer to the substrate and the gap formed between the PE layer and the substrate confirming that growth takes place sideways from the seed; (b) Void formed at the meeting place of two wings.

From Fig. 2 one can notice that the contrast in the wings either side of the seed is practically identical, but there were areas where some small differences could be observed. CBED patterns taken in the areas where some difference in contrast across the wing/wing MF was evident, indicate a twist of about 0.15°. Similar twist misorientation can, occasionally, also be observed at the seed-wing interface; however this twist is not uniform, and there are some regions where no twist (and no dislocation) is present (Fig. 3b). However if PE layers are grown with Si_3N_4 mask structural quality of such layers is much poor and plan view samples show that misorientations of up to 2-3^o between the seed crystal and the wings, or across the meeting-front between adjacent wings [20]. Figure 4 shows a seed region B and adjacent wings A and C, along with the CBED patterns from all three regions. It is clear from the CBED patterns that the wings A and C are similarly oriented and that region B is misoriented from both by roughly 2^o about the (10$\underline{1}$0) axis. One can notice the displacement of the (11$\underline{2}$0) Kikuchi band relative to the central spot (shown by a circle). This angular displacement is described by a series of half loops that have opposite segments in the seed/wing areas.

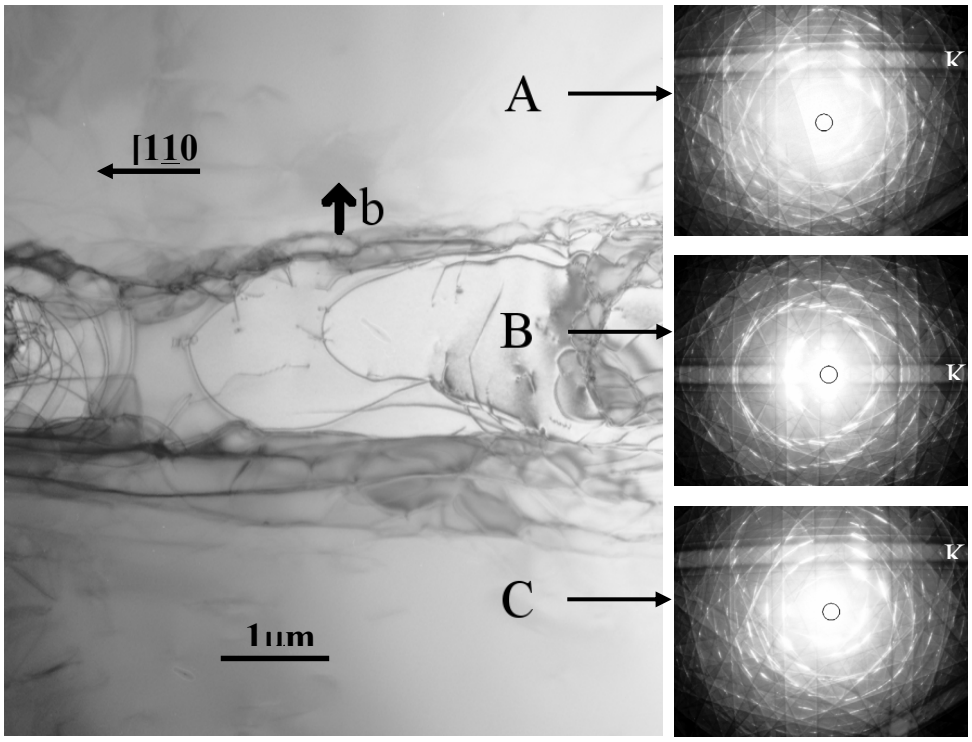

Fig. 4. Plan-view micrograph with the GaN layer grown above silicon nitride mask (B) and adjacent wings (A and C), with CBED patterns from each region, showing the (11$\underline{2}$0) Kikuchi band. Note the different distance between the central beam (marked by circle) and the Kikuchi band, indicating a misorientation.

Fig. 5. TEM micrographs of cross-section uncoalesced pendeo-epitaxial layers grown on a-plane of 4H SiC. High density of defects (mainly stacking faults and dislocations) is observed in the seed area. An inset shows CBED pattern indicating that wider wing is growing with Ga polarity. Bending of dislocations occurs in this wing in the area close to the substrate. A gap between this wing and the substrate is formed for about 500 nm from the original seed and then it starts to touch the substrate. This is shown much clear in (b) which was taken from another wing (magnified). This also shows stacking faults on c-plane (SFc) and on prismatic planes (SFp).

Samples overgrown on non-polar substrates are different. Since the c-plane in these structures is aligned along the growth direction the wings grow in two opposite polar directions. Consistent with earlier studies the growth rate in opposite polar directions [0001] and [000$\underline{1}$] is different, therefore one can expect a different width of the two wings [21]. Figure 5a shows a bright field image of an uncoalesced a-plane PE layer in cross-section. The layers grew to a thickness of 2.7 μm. Indeed one can notice a different width of the 'wings' on the left and right sides of the 'seed' area.

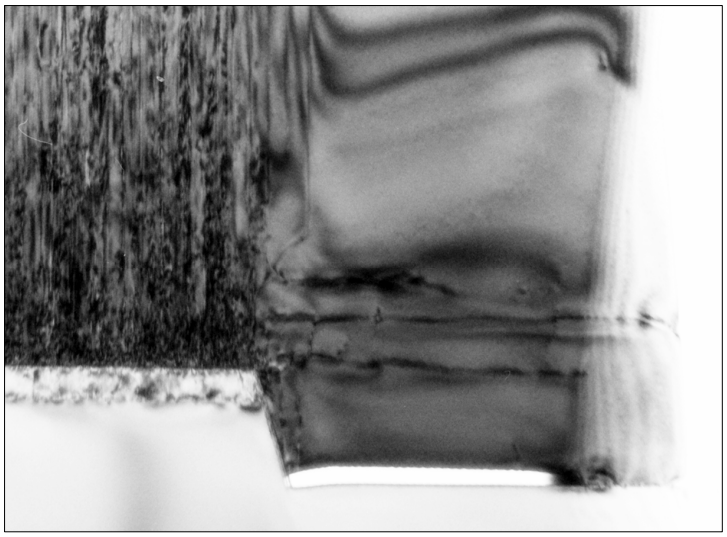

Fig. 6. The micrograph showing a seed area with high defect density and a wing grown with Ga polarity. Note a gap between the wing and the substrate. This gap decreases after the wing reaches the width of about 500 nm. At this point the wing starts to touch the substrate and indicates possible tilting of the wing. Note also a bending of those dislocations which were close to the edge of the seed.

Convergent beam electron diffraction was applied to study growth polarity. The analysis showed 17 times wider wing grown with Ga-polarity (Fig. 5a). When one plans to grow GaN layers with N-polarity, the growth parameters need to be changed in order to obtain a growth rate similar to that observed for growth with Ga-polarity. For overgrowth it is impossible to do it since the two wings grow simultaneously. The resulting structures have wider Ga-polarity wings. Growth of wings starts from the slightly inclined side-walls of the lithographically prepared seeds (SiC+AlN+GaN) and partial side growth starts also from inclined SiC. For a wing grown with Ga polarity one can notice a gap between the overgrown wings and the substrate confirming lateral growth. However when the wing reaches a width of 500 nm it starts to touch the substrate suggesting possible tilt, (Fig. 6). Convergent beam electron diffraction (CBED) taken from a wing area grown with N-polarity (Fig. 7a), central part (seed area) (Fig. 7b), and a wing grown with Ga-polarity (Fig. 7c) show some small tilt and twist. This was also confirmed by Large Angle Convergent Beam Electron Diffraction (LACBED), (Fig. 8). On this figure LACBED patterns were taken from both wings (Figs. 8a and 8c) and the seed area (Fig. 8b). Since this pattern is a superposition of the image and Kikuchi lines a top surface of the uncoalesced area can be easily recognized. If one aligns the surface of the overgrown area from these three areas one can noticed that Kikuchi lines are shifted, especially if one compares the wing grown with N-polarity (Fig. 8a) and the wing grown with Ga-polarity (Fig. 8c). The observed shift indicates a tilt of 1° as well as some twist. It is also easy to see an interaction between the Kikuchi lines and the strain field of dislocations (see Fig. 8a where each dislocation smears the contrast of the Kikuchi line). Since density of dislocations in the seed area is very high Kikuchi lines became almost invisible (Fig. 8b).

Fig. 7. CBED pattern from the wing grown with N-polarity (a), the seed area (b), and the wing grown with Ga-polarity (c). Note a substantial deviation (tilt and twist) in (a) and (b) compared to (c) area.

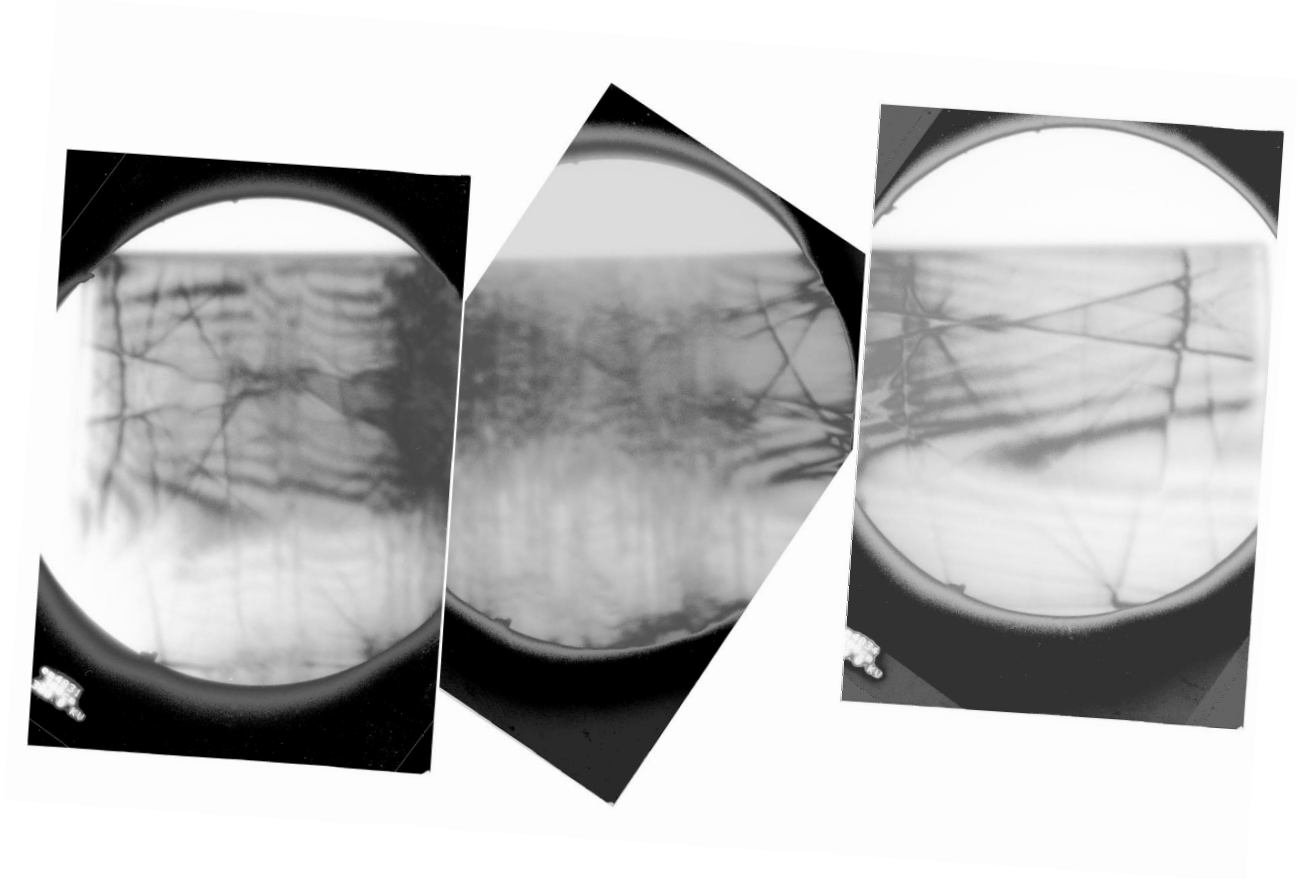

Fig. 8. LACBED pattern from the wing grown with N-polarity (a), the seed area (b), and the wing grown with Ga-polarity (c). Note that Kikuchi lines disappear in the seed area as a result of interaction with defects. Arrows indicate the deviation of the same Kikuchi lines between two wings grown with opposite polarity.

Defects (dislocations and stacking faults formed on the c-plane and on prismatic plane) are present in the seed area and propagate along the growth direction to the sample surface. For defects formed in the wing grown with Ga polarity one can notice that dislocations which were close to the edge of the seed bend and grow parallel to the substrate (Fig. 6). This bending occurs only for dislocations which were close to the seed edge. Dislocations which are further from the seed edge propagate to the sample surface during the growth. A high density of stacking faults can also be observed in the seed area. These faults are mostly associated with the c-plane arranged along growth direction, but there are also stacking faults arranged on prismatic planes. Both of them will be described shortly in the next paragraph. One can noticed that their density drastically decrease in the wing area (Fig. 6) but some prismatic stacking faults are still present in the overgrown wings (Fig. 5b).

Figure 9a shows cross-sectional bright field image of a coalesced sample. The surface of the sample is flat. The sample thickness is 12μm. The stripe width and the stripe period are 2μm and 5μm, respectively. The micrograph reveals voids at areas where two coalesced wings meet each other (meeting fronts (MFs), marked by dashed double-head arrows), similarly as was observed for the coalesced regions for the PE layer grown on c-planes. Very often cracks are observed at MFs (marked by the arrow on Figure 9a). Since wings grown with N polarity are very small, than practically the overgrown areas have mainly Ga-growth polarity and these are the areas where future devices (such as lasers) can be build.

High density of stacking faults formed on the basal plane of hexagonal GaN was observed in cross-sectional TEM images from 'seed' areas. These basal stacking faults (BSFs) are visible in bright field image obtained under two beam condition with $\boldsymbol{g}=1\underline{1}00$ as thin lines arranged perpendicular to the c-direction of the wurtzite GaN (Figure 9b). The measured density of SFs is ~1.3×10^{6}cm^{-1}. Figure 9c represents a bright field image of a 'wing' area obtained with the same two-beam condition as the Figure 9b. One can notice drastic decrease in density of BSFs in the 'wing' areas in comparison to the 'seed' areas. Arrows on the Figure 9c mark two BSFs. Average density of BSFs measured over number of 'wing' areas is ~1.2×10^{4} cm^{-1}.

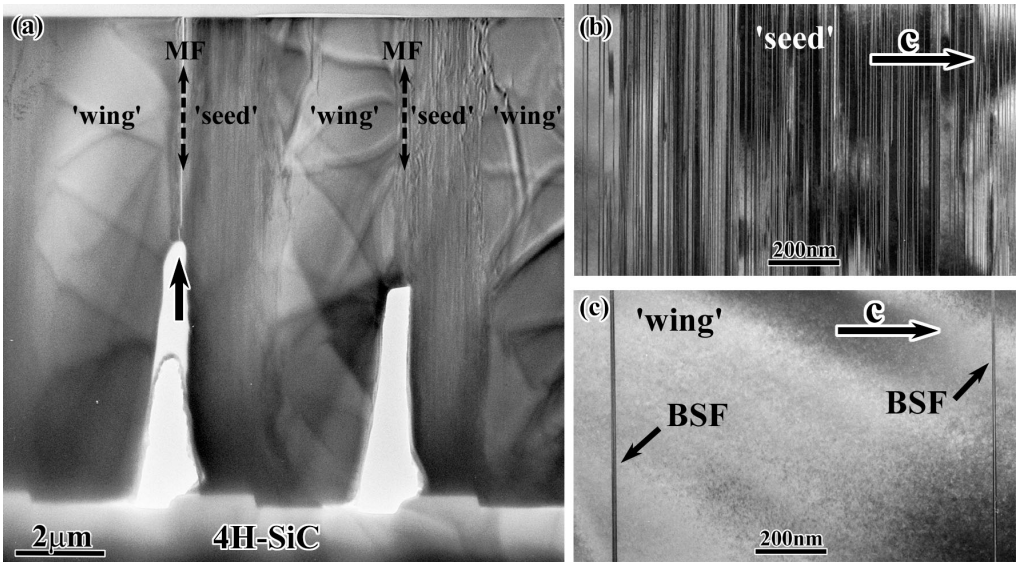

Figure 9. (a) Cross-sectional TEM image of a coalesced a-plane pendeo-epitaxial GaN layer grown on (11$\underline{2}$0) 4H-SiC substrate. Cracks (marked by arrow) are often observed at meeting fronts (MF) of two adjacent 'wings'. Distribution of basal stacking faults in the 'seed' (b) and in the 'wing' areas (c) is shown with higher magnification. Note decrease of basal stacking fault densities in the 'seed' area in comparison to the 'wing' area.

BSFs are also visible in samples prepared in plan-view configuration. Our diffraction contrast experiments have shown that BSFs are in strong contrast for $\boldsymbol{g}=1\underline{1}00$ (Figure 10a), whereas for $\boldsymbol{g}=0002$ contrast from BSFs vanishes (Figure 10b). BSFs are terminated by dislocations (examples are marked by black arrows in Figure 10a). These dislocations with nonzero [000l] component of Burgers vector terminating BSFs are in strong contrast in Figure 10b (marked by black arrows). The density of dislocations reduces by more than two orders of magnitude from ~4.2×10^{10}cm^{-2} in 'seed' areas to ~1.0×10^{8}cm^{-2} in 'wing' areas.

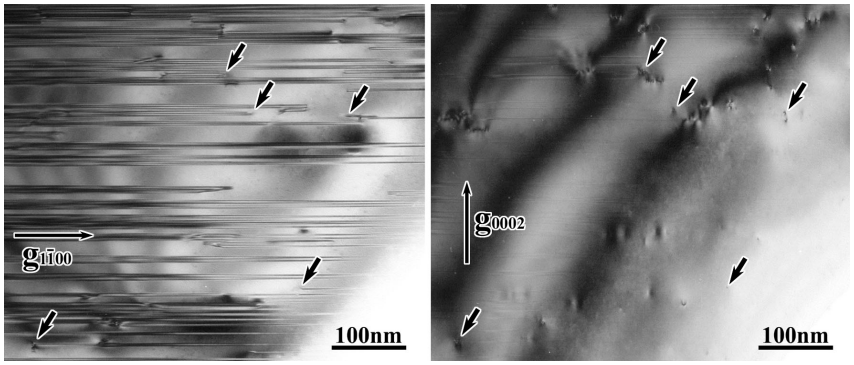

Figure 10. Bright field TEM images of a plan-view sample ('seed' area) obtained with two perpendicular ***g***-vectors: (a) ***g***=1$\underline{1}$00; parallel lines represent stacking faults formed on the basal plane of GaN. (b) ***g***=0002; partial dislocations having a nonzero [0001] component of Burgers vector are in contrast. Black arrows in both images show corresponding places of basal stacking faults terminated by dislocations.

High-resolution transmission electron microscopy (HREM) was applied to determine the nature of BSFs. Three different types of stacking faults formed on the c-plane were found in the seed area: I_1 where…ABABAB… stacking sequence in perfect material is changed to …AB**ABC**BC… (Figure 11a), I_2 with the sequence of…AB**ABCA**CA… (Figure 11b), and I_3 with the sequence of…AB**ABCBA**BA… (Figure 11c). The first two BFSs were bounded by partial dislocations with Burgers vectors ***b***=1/6<20$\underline{2}$3> and ***b***=1/3<1$\underline{1}$00>, respectively, and these stacking faults were found in the seed area and as well in the overgrown ares (wings). The last sequence which corresponds to the I_3 type BSFwere observed only in the 'seed' areas. This type of fault was predicted theoretically and has been shown to have the second lowest formation energy after I_1 type BSF [23].

In addition to BSFs formed on c-planes a different type of faults have been observed on prismatic planes of wurtzite GaN in both the 'seed' and 'wing' areas of studied a-plane PE GaN layers. The fault vectors of these prismatic stacking faults (PSFs) was determined using contrast invisibility criteria. Figure 12a shows a bright field image of a 'wing' area obtained under two beam condition with ***g***=1$\underline{1}$00. The image shows a contrast from two BSFs intersecting with a PSF. The same PSF is out of contrast for images taken with ***g***=$\underline{2}$110, and ***g***=1$\underline{1}$01, respectively (Figures 12b and 12c). Taking also into account that PSFs produce a contrast on images taken with ***g***=3$\underline{3}$00, but not with ***g***=0002 and ***g***=2$\underline{2}$00 (not shown here) their displacement vector should be 1/2[0$\underline{1}$11] [24]. PSFs are always found to intersect with I_1 type BSFs. As fault vectors of a PSF and a BSF are not equal, stair-rod dislocations are present at such intersections.

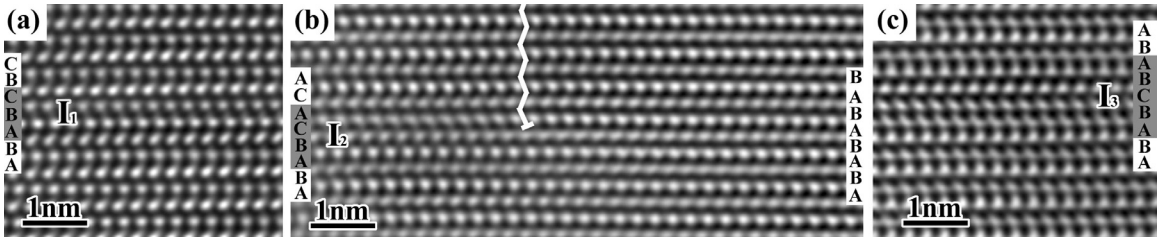

Figure 11. High-resolution images of a plan-view sample show typical stacking faults observed in the sample: (a) I_1 type with stacking sequence …AB**ABC**BC…; (b) I_2 type with stacking sequence …AB**ABCA**CA…. Shockley partial dislocation (***b***=1/3<1$\underline{1}$00>), which terminates the I_2 basal stacking fault is marked in (b); (c) I_3 type with stacking sequence …AB**ABCBA**BA….

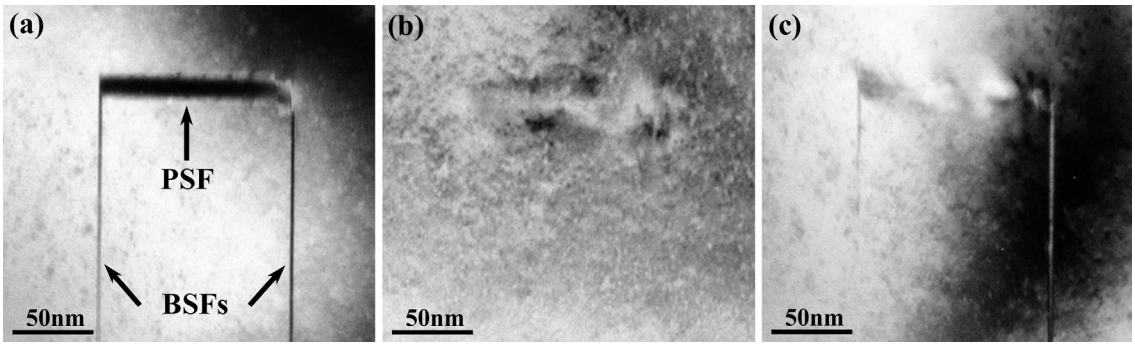

Figure 12. Bright field images of two basal stacking faults intersecting with a prismatic stacking fault obtained under different two beam conditions: (a) $\boldsymbol{g}=1\underline{1}00$, both basal stacking faults and prismatic stacking fault are in contrast. Prismatic stacking fault is out of contrast for (b) $\boldsymbol{g}=0002$, (c) $\boldsymbol{g}=\underline{2}110$ and (d) $\boldsymbol{g}=1\underline{1}01$, respectively.

4. SUMMARY

In summary, we compared two different pendeo-epitaxial samples grown on c-plane and a-plane of SiC. We found that the over-growth on a-plane is much more difficult since the two wings need to grow in two opposite polar directions. Since growth rate in the N- and Ga-polar directions are different and growth of these wings is taking place simultaneously the resulting structures have much wider wings in the Ga-polar direction. For growth in a non-polar direction stacking faults are formed in addition to dislocations since c-planes is arranged along growth direction and formation energy of these faults on these planes are the smallest, In addition to the stacking faults formed on the c-plane prismatic stacking faults were found in both the seed areas and in the wing areas. The study shows that it is much harder to eliminate stacking faults in the overgrown layer in comparison to dislocations, therefore the devices built in these areas will be affected by their presence. However, comparison of the density of defects in the seed area and wing area shows a drastic decrease of the density of defects in the wing area. Due to the fact that in a wing with N-polarity growth is slower it is not easy to make these layers coalesced. In the area of meeting fronts aniphase boundaries could be formed. For the layers grown on polar substrates a high density of dislocations was found at the MFs. These areas need to be avoided for devices build on these materials.

Usually some voids are formed at the meeting fronts between two wings. These are observed independently of growth directions. Formation of these voids can be influenced by impurities collected on the growth fronts of the wings, especially in the areas close to the substrate. In most cases these voids are overgrown. Some tilt and twist between the two wings is observed for both types of overgrowth, in polar and non-polar direction with much smaller misorientation in the latter case. Due to the much smaller growth rate of the wing with N-polarity the overgrown areas have mainly Ga growth polarity.

ACKNOWLEDGMENTS:

This research was supported by AFOSR-ISSA-90-0009.

REFERENCES:

1. S. Yoshida, S. Misawa, and S. Gonda, J. Vac. Sci. Technol. B1, 250 (1983).
2. H. Amano, N. Sawaki, I. Akasaki, and Y. Toyoda, Appl. Phys. Lett. 48, 353 (1986).
3. S. Nakamura, M. Senoh, and T. Mukai, J. Appl. Phys. 30 L1709 (1991).
4. S. Nakamura, M. Senoh, S. Ngahama, N. Iwasa, T. Yamada, T. Matsushida, Y. Sugimoto, and H. Kiyogu, Appl. Phys. Lett. 70. 1417 (1997).
5. B.W. Lim, Q.C. Chen, J.Y. Yang, and M.A. Khan, Appl. Phys. Lett. 68, 3761 (1996).
6. I. Jin Seo, H. Kollmer, J. Off, A. Sohmer, F. Scholz, and A. Hangleiter, Phys. Rev. B 57, R9435 (1998)
7.R. Langer, J. Simon, V. Ortiz, N.T. Pelekanos, A. Barski, R. Andre, and M. Godlewski, Appl. Phys. Lett. 74, 3827 (1999).
8. P. Lefebvre, J. Allegre, B. Gil, H. Mathieu, N. Grandjean, M. Leroux, J. Massies, and P. Bigenwald, Phys. Rev. B 59, 15363 (1999).

9. P. Lefebvre, A. Morel, M. Gallart, T. Taliercio, J. Allegre, B. Gil, H. Mathieu, B. Damilano, N. Grandjean, and J. Massies, Appl. Phys. Lett. 78, 1252 (2001).
10. T. Takeuchi, C. Wetzel, S. Yamaguchi, H. Sakai, H. Amano, I. Akasaki, Y. Kaneko, S. Nakagawa, Y. Yamaoka, and N. Yamada, Appl. Phys. Lett. 73, 1691 (1998).
11. H. Marchand, J.P. Ibbetson, P.T. Fini, P. Kosodoy, S. Keller, S. DenBaars, J.S. Speck, U.K. Mishra, MRS Internet J. Nitride Semicond. Res. 3, 3 (1998).
12. A. Sakai, H. Sunakawa, A. Usui, Appl. Phys. Lett. 71, 2259 (1997).
13. Z. Liliental-Weber, M. Benamara, W. Swider, J. Washburn, J. Park, P. A. Grudowski, C. J. Eiting, and R. D. Dupuis, MRS Internet J. Nitride Semicond. Res. Res. 4S1, G4.6, (1998).
14. Z. Liliental-Weber and D. Cherns, J. Appl. Phys. 89, 7833 (2001).
15. T. Zheleva, S. Smith, D. Thomson, K. Linthicum, P. Rajagopal, R.F. Davis, J. Electr. Mat. 28 (4), L5 (1999).
16. T. Zheleva, S. Smith, D. Thomson, K. Linthicum, P. Rajagopal,, E. Carlson, W. Ashmawi, and R.F. Davis, MRS Internet J. Nitride Semicond. Res. 4S1, G49 (1999).
17. P. Fini, H. Marchand, J.P. Ibbetson, B. Moran, L. Zhao, S.P. DenBaars, J.S. Speck, , U. Mishra Mater. Res. Soc. Symp. Proc. 572, 315 (1999).
18. R.F. Davis, T. Gehrke, K.J. Linthicum, T.S. Zhelewa. E.A. Preble, P. Rajagopal, C.A. Zorman, and M. Mehregany, J. Crystal Growth 225, 134 (2001).
19. Z. Liliental and D. Cherns J. Appl. Phys. **89**, 7833 (2001).
20. Z. Liliental, J. Jasinski, D. Cherns, M. Baines, and R. Davis, Mat. Research. Soc. Symp. 693, 309 (2002).
21. D. N. Zakharov, Z. Liliental-Weber, B. Wagner, Z.J. Reitmeier, E.A. Preble, and R.F. Davis, Mat. Res. Soc. Proc. 798, (Y5.28) 747-52 (2004).
22. D.Hull and D.J. Bacon, in "Introduction to Dislocations" 3rd Ed., Intl. Series on Materials Science and Technology, (Oxford, New York, Beijing, Frankfurt, Sao Paulo, Sydney, Tokyo, Toronto: Pergamon Press, 1984). P. 112.
23. C. Stampfl and C.G. van de walle, Phys. Rev. B 57, R15052 (1998).
24. C.M. Drum, Phil. Mag. 11, 313 (1965).